Synthesis and Properties of Cyclic Ruthenium(II) Porphyrin Tetramers

Kenji Funatsu,[†] Taira Imamura,*[,†] Akio Ichimura,[‡] and Yoichi Sasaki[†]

Division of Chemistry, Graduate School of Science, Hokkaido University, Sapporo 060-0810, Japan, and Department of Chemistry, Faculty of Science, Osaka City University, Osaka 558-0022, Japan

Received July 18, 1997

Tetrameric ruthenium(II) porphyrin complexes, [Ru(4-PyP$_3$P)(CO)]$_4$, **1**, [Ru(4-PyT$_3$P)(CO)]$_4$, **2**, and [Ru(4-PyT$_3$P)(Py)]$_4$, **3**, (4-PyP$_3$P = 5-(4-pyridyl)-10,15,20-triphenylporphyrinato dianion, 4-PyT$_3$P = 5-(4-pyridyl)-10,15,20-tritolylporphyrinato dianion), were self-assembled and were characterized by ^{1}H NMR, IR, and FABMS spectroscopic methods and elemental analyses. The spectroscopic results certified that the ruthenium porphyrin complexes have cyclic tetrameric structures. UV−vis spectra of the tetramers showed broad Soret bands as compared with the respective monomer analogues of Ru(TPP)(CO)(Py) and Ru(TPP)(Py)$_2$. The tetramers **1**−**3** underwent reactions with a large amount of pyridine to give corresponding monomer complexes. Sharpening and increasing intensity in the Soret bands, accompanied by the progress of the monomerization, indicated the presence of the excitonic interactions between cofacially arranged ruthenium porphyrin subunits in these tetrameric molecules. Electrochemical analyses revealed that the first ring-oxidation processes in **1** and **2**, and the oxidation process of Ru(II) to Ru(III) in **3** proceed stepwise.

Introduction

Well-arranged molecules with square or triangle structures have been of great interest in view of supramolecular self-assembly. Square metal complexes (Pt(II),[1] Pd(II),[2] Cd(II),[3] Re(I),[4] Os(VI),[5] Fe(II),[6] Co(II)[7]) were therefore constructed using bridging ligands such as 4,4′-bipyridine and pyrazine, which might recognize or encapsulate other molecules in their nanometeric cavities formed inside in the squares. In fact, the inclusion of organic molecules in the cavities of the Cd(II) square complex or the three-dimensional Pd(II) cagelike complex was realized.[2e,3]

Another area of self-assembling supramolecular chemistry has been developed into unique metal−porphyrin oligomers with oxo,[8] pyridyl,[9] or imidazolyl substituents.[10] Steric controls of angles and lengths in the substituents gave a variety of metal−porphyrin oligomers with cofacial, triangle, or square structures.[9c−f] These porphyrin oligomers elucidated important electronic and photochemical consequences for bacteriochlorophyll (BC) molecules in photosynthetic reaction centers.[9e,10] In many cases, Zn(II) and Mg(II) ions were introduced into the centers of porphyrin rings, because of their excellent photochemical properties and biomimetic implication. Zn(II) and Mg(II) ions are relatively labile metal ions, however, and the metal−porphyrin oligomers are generally in equilibrium between oligomers and monomers in solution. Therefore, we chose an inert metal ion of ruthenium(II) and succeeded in isolating a variety of novel cyclic ruthenium(II) porphyrin tetramers **1**−**3** as shown in Figure 1. Here we report synthesis, characterization, reactivities, and electrochemical properties of the new tetramers.

Results and Discussion

Characterization of Ruthenium Porphyrin Tetramers 1−3. All complexes **1**, **2**, and **3** were sparingly soluble in

[†] Hokkaido University.
[‡] Osaka City University.

(1) (a) Rauter, H.; Hillgeris, E. C.; Erxleben, A.; Lippert, B. *J. Am. Chem. Soc.* **1994**, *116*, 616. (b) Stang, P. J.; Cao, D. H. *J. Am. Chem. Soc.* **1994**, *116*, 4981. (c) Stang, P. J.; Chen, K. *J. Am. Chem. Soc.* **1995**, *117*, 1667. (d) Stang, P. J.; Cao, D. H.; Saito, S.; Arif, A. M. *J. Am. Chem. Soc.* **1995**, *117*, 6273. (e) Manna, J.; Whiteford, J. A.; Stang, P. J.; Muddiman, D. C.; Smith, R. D. *J. Am. Chem. Soc.* **1996**, *118*, 8731. (f) Whiteford, J. A.; Rachlin, E. M.; Stang, P. J. *Angew. Chem., Int. Ed. Engl.* **1996**, *35*, 2524. (g) Stang, P. J.; Cao, D. H.; Chen, K.; Gray, G. M.; Muddiman, D. C.; Smith, R. D. *J. Am. Chem. Soc.* **1997**, *119*, 5163. (h) Plenio, H. *Angew. Chem., Int. Ed. Engl.* **1997**, *36*, 348.

(2) (a) Fujita, M.; Yazaki, J.; Ogura, K. *J. Am. Chem. Soc.* **1990**, *112*, 5645. (b) Fujita, M.; Nagao, S.; Iida, M.; Ogata, K.; Ogura, K. *J. Am. Chem. Soc.* **1993**, *115*, 1574. (c) Stang, P. J.; Zhdankin, V. V. *J. Am. Chem. Soc.* **1993**, *115*, 9808. (d) Fujita, M.; Oguro, D.; Miyazawa, M.; Oka, H.; Yamaguchi, K.; Ogura, K. *Nature* **1995**, *378*, 469. (e) Fujita, M.; Nagao, S.; Ogura, K. *J. Am. Chem. Soc.* **1995**, *117*, 1649. (f) Fujita, M.; Ogura, K. *Bull. Chem. Soc. Jpn.* **1996**, *69*, 1471.

(3) Fujita, M.; Kwon, Y. J.; Washizu, S.; Ogura, K. *J. Am. Chem. Soc.* **1994**, *116*, 1151.

(4) Slone, R. V.; Hupp, J. T.; Stern, C. L.; A-Schmitt, T. A. *Inorg. Chem.* **1996**, *35*, 4096.

(5) Leung, W. H.; Cheng, J. Y. K.; Hun, T. S. M.; Che, C. M.; Wong, W. T.; Cheung, K. K. *Organometallics* **1996**, *15*, 1497.

(6) Romero, M. F.; Ziessel, R.; D-Gervais, A.; Dorsseelaer, A. V. *J. Chem. Soc., Chem. Commun.* **1996**, 551.

(7) Lu, J.; Paliwala, T.; Lim, S. C.; Yu, C.; Niu, T.; Jacobson, A. J. *Inorg. Chem.* **1997**, *36*, 923.

(8) (a) Wojaczynski, J.; Lotas-Grazynski, L. *Inorg. Chem.* **1996**, *35*, 4812. (b) Wojaczynski, J.; Lotas-Grazynski, L. *Inorg. Chem.* **1995**, *34*, 1054. (c) Wojaczynski, J.; Lotas-Grazynski, L. *Inorg. Chem.* **1995**, *34*, 1044. (d) Godziela, G. M.; Tilotta, D.; Goff, H. M. *Inorg. Chem.* **1986**, *25*, 2142. (e) Goff, H. M.; Shimomura, E. T.; Lee, Y. J.; Scheidt, W. R. *Inorg. Chem.* **1984**, *23*, 315. (f) Balch, A. L.; Lotas-Grazynski, L.; Noll, B. C.; Olmstead, M. M.; Zovinka, E. P. *Inorg. Chem.* **1992**, *31*, 2148. (g) Balch, A. L.; Lotas-Grazynski, L.; St. Claire, T. N. *Inorg. Chem.* **1995**, *34*, 1395.

(9) (a) Drain, C. M.; Lehn, J. M. *J. Chem. Soc., Chem. Commun.* **1994**, 2313. (b) Funatsu, K.; Kimura, A.; Imamura, T.; Sasaki, Y. *Chem. Lett.* **1995**, 765. (c) Chi, X.; Guerin, A. J.; Haycock, R. A.; Hunter, C. A.; Sarson, L. D. *J. Chem. Soc., Chem. Commun.* **1995**, 2563. (d) Chi, X.; Guerin, A. J.; Haycock, R. A.; Hunter, C. A.; Sarson, L. D. *J. Chem. Soc., Chem. Commun.* **1995**, 2567. (e) Stibrany, R. T.; Vasudevan, J.; Knapp, S.; Potenza, J. A.; Emge, T.; Schugar, H. J. *J. Am. Chem. Soc.* **1996**, *118*, 3980. (f) Hunter, C. A.; Hyde, R. K. *Angew. Chem., Int. Ed. Engl.* **1996**, *35*, 1936. (g) Yuan, H.; Thomas, L.; Woo, L. K. *Inorg. Chem.* **1996**, *35*, 2808.

(10) (a) Kokube, Y.; Miyaji, H. *J. Am. Chem. Soc.* **1994**, *116*, 4111. (b) Kokube, Y.; Miyaji, H. *Bull. Chem. Soc. Jpn.* **1996**, *69*, 3563.

S0020-1669(97)00884-7 CCC: $15.00
Published on Web 03/17/1998

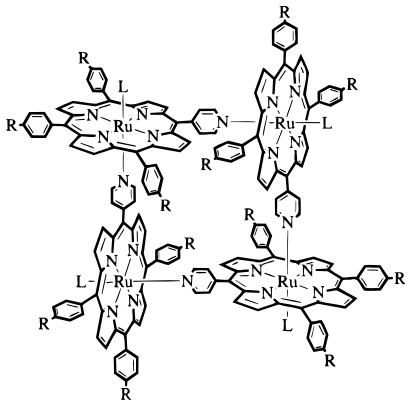

$[Ru(4\text{-}PyP_3P)(CO)]_4$ **1** : R = H, L = CO
$[Ru(4\text{-}PyT_3P)(CO)]_4$ **2** : R = CH_3, L = CO
$[Ru(4\text{-}PyT_3P)(Py)]_4$ **3** : R = CH_3, L = Py

Figure 1. Cyclic ruthenium porphyrin tetramers.

dichloromethane, chloroform, toluene, and benzene, in comparison to the fairly soluble corresponding monomer analogues, Ru(TPP)(CO)(Py) and $Ru(TPP)(Py)_2$.[11] Elemental analyses of **1**, **2**, and **3** were consistent with their respective compositions, as detailed in the Experimental Section. Infrared spectra of **1** and **2** showed characteristic carbonyl stretches at 1956 and 1958 cm^{-1}, respectively. The values of the stretches were almost the same as those of Ru(TPP)(CO)(Py)[12] and of perpendicularly arranged ruthenium porphyrin dimers and trimers reported previously,[13] which indicated the coordination of the carbonyl ligands to ruthenium(II) ions in the tetramers. On the other hand, complex **3** showed no carbonyl stretches, indicating apparently that decarbonylation was completed. FABMS spectra supported the formation of the tetramers of **1**, **2**, and **3**. Respective parent peaks were observed at $(m + 1)/z^+ = 2973$ (8.9% in relative intensity) for **1**, $(m + 1)/z^+ = 3140$ (5.9%) for **2**, and $(m + 1)/z^+ = 3347$ (3.0%) for **3**. In all of the complexes, the deoligomeric peaks corresponding to dimeric and trimeric units were also observed, and the highest peaks in intensity were monomeric units. Although we could not rule out structures of higher nuclearity than tetrameric, similar to the cases of the mass spectra of Fe(III),[8c] Mn(III),[8a] and Ga(III)[8b] oxoporphyrin trimers, ^1H NMR spectra of **1**, **2**, and **3** confirmed the cyclic tetrameric structures.

The ^1H NMR signals of all of the porphyrin oligomers **1**−**3** were assigned as listed in Table 1. The extremely simple spectra of these oligomers showed high symmetry of the framework. Pyridyl and β-pyrrole proton signals experienced very large upfield shifts, as observed previously for some pyridyl porphyrins coordinated perpendicularly to metal porphyrins,[13] and indicated the coordination of ruthenium porphyrin subunits to the axial positions of other ruthenium porphyrin subunits through pyridyl substituents. The β-pyrrole protons were observed as only four signals as listed in Table 1. The integral intensity of each β-pyrrole signal corresponds to eight protons. Pyridyl protons of 2,6 and 3,5 positions were observed as two sets of double doublet peaks distinctly around 1−2 and 5−6 ppm. H−H COSY showed the correlation between 2,6- and 3,5-pyridyl protons, that is, two couplings, between 2,6- and 3,5-pyridyl protons in upper field and between the protons in lower field were observed (Figure S1). The integral intensity of each pyridyl proton signal was equivalent to four protons. These results indicated that each ruthenium porphyrin subunit in the oligomeric framework is equivalent and that one set of the 2,6 and 3,5 protons in each pyridyl group of a porphyrin subunit is faced to the outer sphere of the framework and the other set of the protons is directed toward the center of the framework. In the case of **3**, axial pyridine signals were also observed at 2.32, 4.97, and 5.84 ppm in a higher region than that of an ordinary free pyridine (7−9 ppm). Furthermore, the number of the ruthenium porphyrin subunits composing the oligomers was confirmed to be 4 from the ratios between integral intensities in each signal for **1**−**3** and those for a standard amount of a free base porphyrin, H_2TPP or H_2TTP. In addition, the right angle (90°) between N(Py)−Ru and the ruthenium porphyrin plane rules out the formation of other cyclic oligomers such as trimers and pentamers which must have significant strains in coordination spheres. The spectral and topological observations apparently indicated that the products were cyclic porphyrin tetramers.

UV−vis Spectral Studies. Both UV−vis spectra of **1** and **2** in dichloromethane showed an intense Soret band at 412 nm and two Q-bands at 532 and 568 nm, similarly to that of Ru(TPP)(CO)(Py)[14] as listed in Table 2. However, the Soret bands of **1** and **2** (half-width = 28 nm) are relatively broad compared to that of Ru(TPP)(CO)(Py) (half-width = 18 nm), and their molar absorptivities of the tetramers were significantly smaller (ca. 80×10^4 M^{-1} cm^{-1}) for the four Ru(TPP)(CO)(Py) (ca. $28 \times 4 \times 10^4$ M^{-1} cm^{-1}).[14] Some perpendicularly linked metal porphyrin dimers exhibited no broadening of the Soret band.[13] Hence the broadening of the Soret bands of **1** and **2** must result from the excitonic interactions between two ruthenium porphyrin subunits aligned parallel. The UV−vis spectral changes accompanied by the cleavage of the tetramer core to the corresponding monomers confirmed the construction of these tetramers, that is, the addition of pyridine to the dichloromethane solutions of the tetramers generated the corresponding monomers, $Ru(4\text{-}PyP_3P)(CO)(Py)$ and $Ru(4\text{-}PyT_3P)(CO)(Py)$, as observed by the sharpening and increasing intensity of the Soret bands as shown in Figure 2. The final spectra of **1** and **2**, with half-widths of 18 nm and molar absorptivities of about 110×10^4 M^{-1} cm^{-1} (27.5×10^4 M^{-1} cm^{-1} per one subunit), were almost the same as that of Ru(TPP)(CO)(Py). The Soret band of **3** was also broad in comparison to the corresponding monomer of $Ru(TPP)(Py)_2$ and it also exhibited the sharpening and increasing intensity of the Soret band in the process of generating the monomer of $Ru(4\text{-}PyT_3P)(Py)_2$.

Electrochemical Properties. All of the tetrameric ruthenium porphyrin complexes showed two oxidation stages, each of which involved four electrons. Redox potentials for the oxidation processes of **1**, **2**, and **3** are summarized in Table 3. Cyclic voltammograms and the simulation charts of **2** and **3** are shown in Figure 3.

The four-electron oxidized species of **1** and **2** at the first oxidation stages, generated by bulk electrolysis at 1.0 V, showed broad bands around 770 and 500−700 nm in the visible region as shown in Figure 4. The spectra are characteristic of the cation radicals of porphyrin rings, as observed in the monomeric Zn^{II},

(11) Abbreviations: Py = pyridine, TPP = 5,10,15,20-tetraphenylporphyrinato dianion, $4\text{-}PyP_3P$ = 5-(4-pyridyl)-10,15,20-triphenylporphyrinato dianion, $4\text{-}PyT_3P$ = 5-(4-pyridyl)-10,15,20-tritolylporphyrinato dianion.

(12) Little, R. G.; Ibers, J. A. *J. Am. Chem. Soc.* **1973**, *95*, 8583.

(13) (a) Funatsu, K.; Kimura, A.; Imamura, T.; Ichimura, A.; Sasaki, Y. *Inorg. Chem.* **1997**, *36*, 1625. (b) Kariya, N.; Imamura, T.; Sasaki, Y. *Inorg. Chem.* **1997**, *36*, 833.

(14) Bonnet, J. J.; Eaton, S. S.; Holm, R. H.; Ibers, J. A. *J. Am. Chem. Soc.* **1973**, *95*, 2141.

Table 1. Chemical Shift Values of Ruthenium(II) Porphyrin Oligomers in $CDCl_3$ at 23 °C (δ/ppm vs TMS)

complex	2,6-py	3,5-py	β-pyrrole	*o*-phenyl	*m*,*p*-phenyl	CH_3 (tolyl)	py (axial ligand)
[Ru(4-PyP$_3$P)(CO)]$_4$, **1**	0.96	5.72	6.97, 8.23	7.87	7.70		
	1.71	6.03	8.57, 8.65	8.12			
[Ru(4-PyT$_3$P)(CO)]$_4$, **2**	0.95	5.68	6.90, 8.25	7.77	7.47	2.62	
	1.68	5.99	8.59, 8.65	8.03		2.71	
[Ru(4-PyT$_3$P)(Py)]$_4$, **3**	0.93	5.67	6.65, 7.77	7.70−7.90	7.26−7.42	2.57	α: 2.32
	1.91	5.78	8.06, 8.12			2.65	β: 4.97
							γ: 5.84

Table 2. UV−Vis Data of Ruthenium Porphyrin Tetramers in CH_2Cl_2 at 23 °C

complex	λ_{max}/nm (ϵ; 10^4 M^{-1} cm^{-1}/ϵ per porphyrin subunit)
[Ru(4-PyP$_3$P)(CO)]$_4$, **1**	412 (78.0/19.5), 532 (6.10/1.53), 569 (sh)
[Ru(4-PyT$_3$P)(CO)]$_4$, **2**	412 (80.4/20.1), 533 (7.45/1.86), 570 (sh 2.37/0.60)
[Ru(4-PyT$_3$P)(Py)]$_4$, **3**	408 (47.9/12.0), 506 (8.59/2.15), 536 (sh 2.77/0.69), 585 (sh 1.59/0.40), 668 (sh 0.76/0.19)

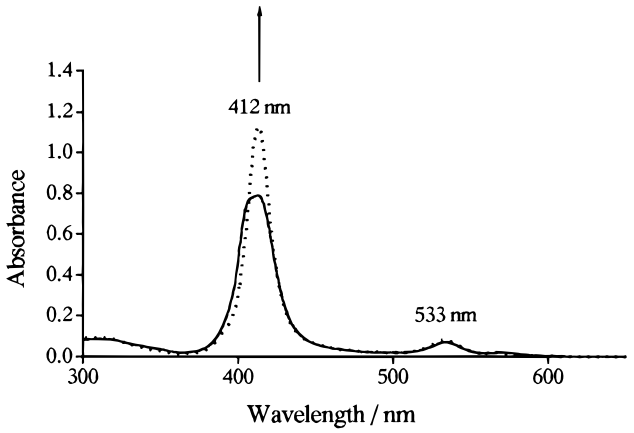

Figure 2. UV−vis spectral change accompanied by the addition of an excess amount of pyridine to the dichloromethane solution of **2** at 25 °C.

Co^{III}, and Ru^{II}(CO) porphyrin complexes.[15,16] Thus, the first four-electron oxidation in **1** and **2** occurs at the porphyrin rings, not at the ruthenium ions. Of particular interest is Figure 3a, which shows a broad redox wave of the first oxidation stage. To deconvolute the wave of the first stage, simulation of the cyclic voltammogram was carried out. The simulated voltammogram in Figure 3b was well-fitted with the experimental curve. The results reveal that the first ring oxidation wave consists of four stepwise one-electron oxidations, as listed in Table 3. The simulated voltammogram gives the respective redox potentials, $E^{\circ\prime}_1$. This oxidation behavior indicates the presence of a little interaction between the ruthenium porphyrin subunits in each tetramer; otherwise, the first oxidation stage would give a simple oxidation wave involving four electrons with the peak separation of 59 mV.[17] In comparison to the $E^{\circ\prime}_1$ values in **2**, the corresponding $E^{\circ\prime}_1$ values in **1** are slightly more positive. This reflects the less electron-withdrawing ability of the meso substituents in **1**. However, there are no essential differences between **1** and **2** in both $\Delta E^{\circ\prime}$ (the potential difference between neighboring one-electron oxidation steps) and $\Delta E^{\circ\prime}_{total}$ (the potential difference between the first and fourth oxidation steps) in the first oxidation stages.

The second oxidation stage for **1** and **2** gave a one-step four-electron wave with an anodic and cathodic peak potential separation of 59 mV and was also assigned to the porphyrin ring-centered oxidations as in the Ru(TPP)(CO)(Py) system.[15] This result indicates that there is no interaction between the porphyrin monocation subunits which are independently oxidized to give the porphyrin dication subunits. This is in contrast to the first ring oxidation process.

Tetramer **3** exhibited a redox behavior different from those of complexes **1** and **2**. The first four-electron oxidation occurred at the central ruthenium ions rather than at the porphyrin rings, as observed in the corresponding monomer of Ru(TPP)(Py)$_2$.[15] The oxidation of the ruthenium centers also proceeds stepwise as shown in Figure 3c. The simulated voltammogram agrees well with the experimental curve, as shown in Figure 3d, and then gives the each redox potential of Ru(III/II), $E^{\circ\prime}_{Ru}$. The second four-electron oxidation process, which is the first porphyrin ring-centered oxidation in **3**, occurred without interactions between the subunits, similarly to the second porphyrin oxidation stage of **1** and **2**. The potential difference of $\Delta E^{\circ\prime}_{total}$, which is a measure of the extent of overall interaction between the ruthenium centers of **3,** is 117 mV. The value is almost the same as those of **1** (136 mV) and **2** (128 mV), though the oxidation moieties at the first oxidation stages are different between **1** or **2** and **3**.

Cleavage of the Tetrameric Structures. As described above, treatments of **1**−**3** with excess pyridine result in the formation of the corresponding monomeric pyridine derivatives. In the processes of pyridine substitutions, a significant increase in intensity of the Soret bands was observed. The pyridine substitutions of **1** and **2** proceeded readily even at 25 °C in pyridine−dichloromethane solutions, possibly because of the trans effect of strong π-acid carbonyl ligands. On the other hand, the reaction of **3** required high temperatures even in neat pyridine. The slow pyridine exchange is also observed for the reactions of a monomeric Ru(TPP)(Py)$_2$ and a picnic basket analogue of Ru(C6-PBP)(Py)$_2$.[18]

The depolymerization reactions were followed by UV−vis spectrometry under a large excess of pyridine. In the tetramer of **2**, the reaction was completed within 15 min when the concentration of **2** was 1.24×10^{-6} M in the 3.71×10^{-3} M pyridine−dichloromethane solution. The kinetics obeyed a pseudo-first-order rate law for the systems with variable concentrations of excess pyridine. Change in the initial concentration of **2** over a factor of 5 gave no difference in the observed first-order rate constants at a given concentration of pyridine. The second-order rate constant obtained by the plots of the pseudo-first-order rate constants against the concentration of pyridine was evaluated to be $(2.1 \pm 0.1) \times 10^{-1}$ M^{-1} s^{-1}. The observation suggests that the first cleavage of the cyclic structure to generate an intermediate with chain or zigzag structures may be rate-controlling, and the successive steps of

(15) (a) Brown, G. M.; Hopf, F. R.; Ferguson, J. A.; Meyer, T. J.; Whitten, D. G. *J. Am. Chem. Soc.* **1973**, *95*, 5939. (b)Felton, R. H. In *The Porphyrins*; Dolphin, D., Ed.; Academic Press: New York, 1979; Vol. 5, Chapter 3.
(16) Wolberg, A.; Manassen, J. *J. Am. Chem. Soc.* **1970**, *92*, 2982.
(17) Flanagan, J. B.; Margel, S.; Bard, A. J.; Anson, F. C. *J. Am. Chem. Soc.* **1978**, *100*, 4248.
(18) Collman, J. P.; Brauman, J. I.; Fitzgerald, J. P.; Abers, J. A. *J. Am. Chem. Soc.* **1988**, *110*, 3486.

Table 3. Redox Potentials ($E^{\circ\prime}$) and the Potential Differences ($\Delta E^{\circ\prime}$) of the Ruthenium Porphyrin Tetramers

	first oxidn stage[a]			second oxidn stage
complex	Ru(III/II) $E^{\circ\prime}_{Ru}$, mV ($\Delta E^{\circ\prime}$, mV)	first ring oxidn $E^{\circ\prime}_1$, mV ($\Delta E^{\circ\prime}$, mV)	$\Delta E^{\circ\prime}_{total}$, mV	ring oxidn $E^{\circ\prime}_2$, mV
[Ru(4-PyP$_3$P)(CO)]$_4$, **1**		766 (28) 794 (48) 842 (60) 902	136	1311
[Ru(4-PyT$_3$P)(CO)]$_4$, **2**		735 (18) 753 (49) 802 (61) 863	128	1281
[Ru(4-PyT$_3$P)(Py)]$_4$, **3**	95 (69) 164 (23) 187 (25) 212		117	1217
Ru(TPP)(CO)(Py),[b] (vs SSCE)		810	0	1360
Ru(TPP)(Py)$_2$,[b] (vs SSCE)	210		0	1260

[a] $E^{\circ\prime}$ were deduced by CV simulation. [b] Reference 15.

the breaking of the chains to form monomers are relatively fast. ^{1}H NMR spectral changes during the reaction processes do not contradict the above mechanism; that is any signals derived from the oligomers with noncyclic structures were not observed.

The cleavage reaction of **3** also progressed in neat pyridine (12.4 M) solution. The apparent increase in the intensity of the Soret band was completed in about 70 min at 110 °C as shown in Figure 5. The first-order rate constant (k_{obs}) was 5.1 $\times$ 10^{-4} s^{-1} at 110 °C and 1.9 $\times$ 10^{-5} s^{-1} at 90 °C. The reaction was also followed by the ^{1}H NMR method for the deuterated pyridine solutions (Figure S2). At room temperature, the proton signals of 3,5-pyridyl, β-pyrrole, and γ-pyridine of axial pyridine ligands exhibited no change over a few weeks.[19] At 90 °C, the 3,5-pyridyl and β-pyrrole proton signals of the cyclic structure exhibited essentially no change, except for broadening (as compared with the signal at room temperature) of 3,5-pyridyl proton signals due to the rotation of the pyridyl groups (Figure S2).[20,21] Thus the signal of 3,5-pyridyl protons cannot be used for the estimation of the depolymerization reaction. The prompt decay of the γ-proton signal of the axial pyridine (C_5H_5N) must be due to the replacement with deuterated pyridine at 90 °C. The results supported that the cyclic tetrameric structures are energetically and topologically robust.

Hunter and co-workers discussed the stability of cyclic tetrameric structure on the basis of the UV−vis spectroscopic studies.[9c,d] Cyclic zinc porphyrin dimer, trimer, and tetramer were constructed by self-assembling through a variety of pyridyl substituents linking at the end of meso peptide substituents.[9c,d] From the UV−vis absorption dilution studies for the zinc porphyrin tetramer, they concluded that cyclic tetrameric structure is the major component of the zinc porphyrin oligomers and that the chain ones are negligible. They also suggested that the zinc porphyrin oligomers [Zn(4-PyP$_3$P)]$_n$ reported by Fleischer and Shachter[22] have cyclic tetrameric structures. However, the ^{1}H NMR spectrum of [Zn(4-PyP$_3$P)]$_n$ exhibiting broad single signals for both 2,6- and 3,5-pyridyl and the most upfield shifted β-pyrrole protons around 2, 6, and 7.5 ppm, respectively,[22] is entirely different from that of [Ru(4-PyP$_3$P)(CO)]$_4$. Variable temperature ^{1}H NMR measurements of [Zn(4-PyP$_3$P)]$_4$ by us clarified the problem as shown in Figure 6. When the temperature was lowered to −40 from 25 °C, the broad pyridyl signals were changed to two sets of apparent peaks. The spectrum at −40 °C is the same as that of [Ru(4-PyP$_3$P)(CO)]$_4$, that is, two sets of double doublet pyridyl signals and sharp four β-pyrrole signals as observed in the ruthenium tetramer systems. Thus it was concluded that the fast exchange, relative to NMR time scale, between cyclic and chain structures occurred in the case of [Zn(4-PyP$_3$P)]$_4$ with the concentrations for the ^{1}H NMR measurement at room temperature and that the cyclic tetramer is the major component at low temperature.

(19) 2,6-Pyridyl proton signals were obscured by the signals of impurities contained in deuterated pyridine.

(20) Sandström, J. In *Dynamic NMR Spectroscopy*; Academic Press: London, New York, 1982; pp 93−123. 3,5-Pyridyl proton signals of **1**, **2**, and **3** were coalesced at 378, 379, and 364 K in deuterated toluene solutions, respectively, because of the rotation of the pyridyl rings at high temperatures.[9b] However, the β-pyrrole protons of **1**−**3** kept four sharp signals, indicating no cleavage of the cyclic framework even at high temperatures. Free energies of activation for the rotations in **1**−**3** were approximately estimated to be the same value of 18 kcal mol^{-1}. The value is comparable to the rotation barriers (E_A) of orthounsubstituted phenylporphyrins (15−18 kcal mol^{-1}).[14,15] Free energies of activation for the exchange in **1**−**3** were estimated:

$$\Delta G^{\ddagger} = 4.57\, T_c(10.32 + \log T_c - \log k_c) \quad (1)$$

where T_c (K) is the coalescence temperature of two 3,5-pyridyl signals and k_c is the rotating rate at T_c. k_c, defined in eq 2, is the rotation rate at the coalescence temperatures:

$$k_c = \pi(\Delta\nu)/2 \quad (2)$$

where $\Delta\nu$ (Hz) is the chemical shift difference between two 3,5-pyridyl signals. The temperatures of T_c were 378, 379, and 364 K for **1**, **2**, and **3**, respectively, and the values of $\Delta\nu$ of **1**, **2**, and **3** were 72.9, 78.3, and 29.7 Hz, respectively.

(21) (a) Sessler, J. L.; Johnson, M. R.; Creager, S. E.; Fettinger, J. C.; Ibers, J. A. *J. Am. Chem. Soc.* **1990**, *112*, 9310. (b) Eaton, S. S.; Eaton, G. R. *J. Am. Chem. Soc.* **1977**, *99*, 6594. (c) Eaton, S. S.; Eaton, G. R. *J. Am. Chem. Soc.* **1975**, *97*, 3660.

(22) Fleischer, E. B.; Shachter, A. M. *Inorg. Chem.* **1991**, 30, 3763.

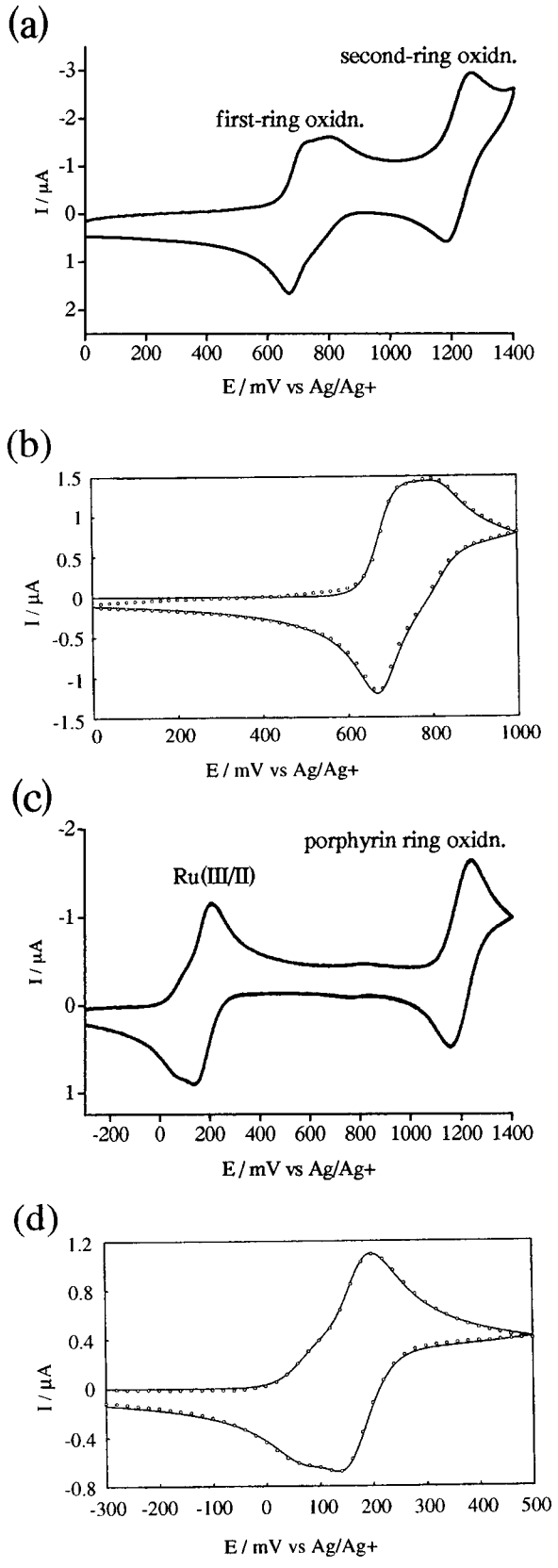

Figure 3. (a) Cyclic voltammogram of **2** in 0.1 M TBA(PF_6)−CH_2Cl_2 at 10 °C. (b) Simulation of the cyclic voltammogram of **2**. The dotted line (∘∘∘) is the experimental curve, and the solid line (—) is the simulation curve. (c) Cyclic voltammogram of **3** in 0.1 M TBA(PF_6)−CH_2Cl_2 at 10 °C. (d) Simulation of the cyclic voltammogram of **3**. The dotted line (∘∘∘) is the experimental curve, and the solid line (—) is the simulation curve.

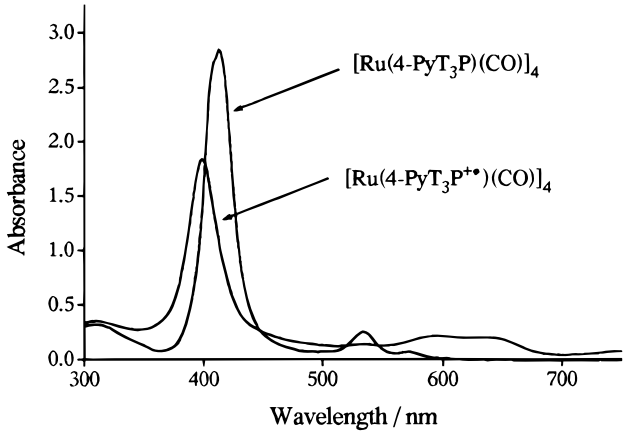

Figure 4. UV−vis spectra of $[Ru(4\text{-}PyT_3P)(CO)]_4$, **2**, and $[Ru(4\text{-}PyT_3P^{+\bullet})(CO)]_4$ in 0.1 M TBA(PF_6)−CH_2Cl_2 at 23 °C.

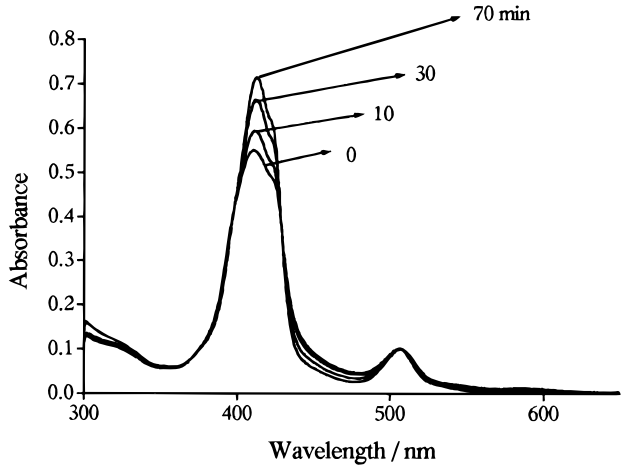

Figure 5. UV−vis spectral change of **3** in pyridine at 110 °C.

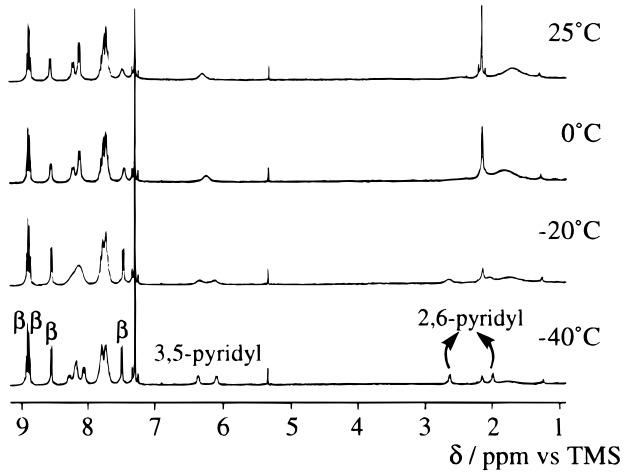

Figure 6. Variable temperature ^1H NMR spectra of $[Zn(4\text{-}PyP_3P)]_n$ in $CDCl_3$.

If $[Zn(4\text{-}PyP_3P)]_n$ was recrystallized under cold conditions, cyclic zinc porphyrin tetramer could be isolated.

Conclusions

New three-dimensional cyclic ruthenium porphyrin tetramers **1**−**3** were synthesized and characterized. Variable temperature ^1H NMR measurements and kinetic studies with UV−vis and NMR methods revealed that the cyclic tetrameric structures are stable energetically and topologically. UV−vis spectra of **1**−**3** showed broad Soret bands. The Soret bands were sharpened

and increased in intensity by the generation of corresponding monomers in the process of pyridine substitution reactions. The results demonstrated the presence of excitonic interactions between the ruthenium porphyrin subunits aligned parallel in the tetramer frameworks. Redox behaviors of the cyclic tetramers were characteristic. The first four ring oxidations of **1** and **2**, and the oxidation of four ruthenium ions of **3** proceeded stepwise. The extent of overall splitting of the first redox processes of all of the complexes was almost the same (ca. 120 mV).

Experimental Section

Materials. Pyrrole, benzaldehyde, *p*-tolualdehyde, and 4-pyridinecarbaldehyde for preparations of the porphyrins, H_2(4-Py)P_3P and H_2-(4-Py)T_3P, were purchased from Wako and used without further purification. Triruthenium(0) dodecacarbonyl, $Ru_3(CO)_{12}$, was purchased from Aldrich. Methanol was purified by distillation under N_2 gas after dehydration using 4-Å molecular sieves. Dichloromethane and toluene were used without further purification. Silica gel (Wakogel C-300) and alumina (Wolem, neutral, activity III) were used for column chromatography. TLC silica plates were purchased from Tokyo Kasei.

Measurements. ^{1}H NMR spectra were recorded on a JEOL-EX270 spectrometer. IR spectra (KBr method) were measured with a Hitachi 270-50 infrared spectrophotometer. UV−vis spectra were recorded on a Hitachi U-3410 spectrophotometer or a Hitachi U-3000 spectrophotometer. Cyclic voltammetry was performed with a BAS CV-50W voltammetry analyzer. The data were digitized and stored in a connecting personal computer. The working and the counter electrodes for the cyclic voltammetric measurements were a platinum disk (i.d. = 1.6 mm) and a platinum wire. Cyclic voltammograms were recorded at a scan rate of 100 mV/s at 10 °C. The sample solutions in CH_2Cl_2 containing 0.1 M (TBA)PF_6·CH_2Cl_2 ((TBA)PF_6 = tetrabutylammonium hexafluorophosphate) were deoxygenated by argon stream. The reference electrode was Ag/0.01 M [Ag($CH_3CN)_2$]PF_6, 0.1 M (TBA)-PF_6 (acetonitrile). The potentials reported here are with respect to this reference electrode, against which the redox potential of ferrocenium−ferrocene was 0.352 V. Digital simulation of cyclic voltammograms was performed on a simulation software DigiSim from Bioanalytical Systems (BAS). The visible kinetic measurements were perfomed on a Hitachi U-3000 spectrophotometer with a thermostated cell holder, for example, 2.5 mL of dichloromethane solutions of [Ru(4-PyT$_3$P)-(CO)]$_4$, **2** (1.244×10^{-6} M and 2.184×10^{-7} M), were kept in the cell holder thermostated at 25 °C at least for 10 min before the additions of 8.3−25 mL of 3.71×10^{-1} M pyridine−dichloromethane solution. The absorbance change at 412 nm was monitored with time and analyzed by plotting $\ln[(A_\infty - A_t)/(A_\infty - A_0)]$ versus time (s), where A_0 is the initial absorbance, A_∞ is the absorbance at infinite time, and A_t is the absorbance at time, t. In the case of [Ru(4-PyT$_3$P)(Py)]$_4$, **3**, the pyridine solutions were equilibrated for 10 min at 110 °C. The UV−vis spectra from 300 to 800 nm were scanned until no further changes were observed. Analyses of the absorbance changes at 412 nm were carried out by plotting $\ln[(A_\infty - A_t)/(A_\infty - A_0)]$ versus time (s), similarly to the [Ru(4-PyT$_3$P)(CO)]$_4$, **2**, system.

Synthesis of H_2(4-Py)P_3P and H_2(4-Py)T_3P. Porphyrins containing *meso*-pyridyl groups were synthesized by using the literature method.[22]

H_2(4-Py)P_3P. The mixed solution of benzaldehyde (15 mL), 4-pyridinecarbaldehyde (5 mL), and pyrrole (14 mL) was refluxed in propionic acid. The crystalline product of the porphyrin mixture (5.18 g) was obtained after cooling the solution. The desired porphyrin was isolated from the porphyrin mixture by silica gel column chromatography. The amount of H_2(4-Py)P_3P was 1.44 g, which corresponds to 28% of the total yield of the porphyrin mixture. The purified porphyrins were identified by thin-layer chromatography, elemental analysis, and ^{1}H NMR measurements. These data agreed well with the reported results.[22] Anal. Calcd for $C_{43}H_{29}N_5$: C, 83.88; H, 4.75; N, 11.38. Found: C, 83.82; H, 4.83; N, 11.13. ^{1}H NMR (CD_2Cl_2, 400 MHz): H_{NH} −2.88 (s, 2H), H_β 8.85 (m, 8H), H_o 8.20 (m, 6H), $H_{m,p}$ 7.77 (m, 9H), $H_{2,6-Py}$ 8.98 (dd, 2H), $H_{3,5-Py}$ 8.15 (dd, 2H) ppm.

H_2(4-Py)T_3P. H_2(4-Py)T_3P was synthesized by a method similar to that of H_2(4-Py)P_3P using *p*-tolualdehyde in place of benzaldehyde. *p*-Tolualdehyde (15 mL), 4-pyridinecarbaldehyde (5 mL), and pyrrol (15 mL) were used. Crystalline product of the porphyrin mixture was obtained (4.98 g). The amount of H_2(4-Py)T_3P was 1 g. Yield: 20%. Anal. Calcd for $C_{46}H_{35}N_5$: C, 83.99; H, 5.36; N, 10.65. Found: C, 83.81; H, 5.29; N, 10.30. ^{1}H NMR ($CDCl_3$, 270 MHz): H_{NH} −2.79 (s, 2H), H_{CH_3} 2.70 (s, 9H), H_β 8.87 (m, 8H), H_o 8.08 (d, J = 8.1 Hz, 6H), H_m 7.55 (d, J = 8.1 Hz, 6H), $H_{2,6-Py}$ 9.02 (dd, 2H), $H_{3,5-Py}$ 8.16 (dd, 2H) ppm.

Synthesis of Tetramers. [Ru(4-PyP$_3$P)(CO)]$_4$, 1. Procedure 1. A benzonitrile solution (100 mL) containing $Ru_3(CO)_{12}$ (200 mg, 3.13×10^{-4} mol) and H_2(4-Py)P_3P (200 mg, 3.25×10^{-4} mol) was heated under reflux for 12 h. The solution was filtered through a sintered glass followed by evaporation to dryness. The resulting solid was dissolved in a small amount of dichloromethane and separated by silica gel column chromatography with dichloromethane as an eluent. The first eluted red band was collected and evaporated to dryness. The solid product was recrystallized from dichloromethane-methanol and dried at 100 °C in vacuo for 5 h. Yield: 48 mg, 20%.

Procedure 2. A diethylene glycol monomethyl ether suspension (100 mL) containing H_2(4-Py)P_3P (100 mg, 1.66×10^{-4} mol) and Ru_3-$(CO)_{12}$ (100 mg, 1.56×10^{-4} mol) was refluxed for 2 h under N_2 atmosphere. The reaction was monitored by visible spectroscopy, and heating was stopped when the characteristic band of H_2(4-Py)P_3P around 650 nm was no longer observed. To the cooled and filtered solution, was added 100 mL of a saturated NaCl aqueous solution. The resulting precipitate was removed by filtration through a sintered glass, washed with water, and dried at 100 °C in vacuo for 1 h. The crude product exhibited a band around 600 nm, because of a chlorine impurity. Hence, oxidation of the crude products by DDQ (2,3-dichloro-5,6-dicyano-1,4-benzoquinone) was carried out.[23] An excess amount of DDQ was added to the dichloromethane solution of the crude product, and the suspension was stirred at room temperature until the characteristic band around 600 nm disappeared. The suspension was filtered. The filtrate was chromatographed on a silica gel column using toluene as an eluent. The first eluted band was collected and evaporated to dryness. The solid product was recrystallized from dichloromethane−methanol and dried at 100 °C in vacuo for 5 h. Yield: 30 mg, 25%. Anal. Calcd for $C_{176}H_{108}N_{20}O_4Ru_4$: C, 71.14; H, 3.66; N, 9.43. Found: C, 71.55; H, 4.36; N, 9.33. ^{1}H NMR (CD_2Cl_2, 270 MHz): $H_{2,6-Py}$ 0.96 (d, 5.94 Hz, 4H), 1.71 (d, 5.94 Hz, 4H), $H_{3,5-Py}$ 5.72 (dd, 5.94, 1.65 Hz, 4H), 6.03 (dd, 5.94, 1.65 Hz, 4H), H_β 6.97 (d, 4.95 Hz, 8H), 8.23 (d, 4.95 Hz, 8H), 8.57 (d, 4.95 Hz, 8H), 8.65 (d, 4.95 Hz, 8H), H_o 7.87, 8.12 (m, 24H), $H_{m,p}$ 7.70 (m, 36H) ppm.

[Ru(4-PyT$_3$P)(CO)]$_4$, 2. For the preparation of [Ru(4-PyT$_3$P)(CO)]$_4$, procedures 1 and 2 for **1** were also employed using H_2(4-Py)T_3P in place of H_2(4-Py)P_3P. $Ru_3(CO)_{12}$ (150 mg, 2.35×10^{-4} mol) and H_2-(4-Py)T_3P (100 mg, 1.56×10^{-4} mol) were used. Yield: 20 mg, 17%. Anal. Calcd for $C_{188}H_{132}N_{20}O_4Ru_4$: C, 71.92; H, 4.24; N, 8.92. Found: C, 71.67; H, 4.81; N, 9.06. ^{1}H NMR ($CDCl_3$, 270 MHz): $H_{2,6-Py}$ 0.95 (d, 5.94 Hz, 4H), 1.68 (d, 5.94 Hz, 4H), $H_{3,5-Py}$ 5.68 (dd, 5.94, 1.65 Hz, 4H), 5.99 (dd, 5.94, 1.65 Hz, 4H), H_β 6.90 (d, 4.95 Hz, 8H), 8.25 (d, 4.95 Hz, 8H), 8.59 (d, 4.95 Hz, 8H), 8.65 (d, 4.95 Hz, 8H), H_o 7.77, 8.03 (m, 24H), H_m 7.47 (m, 24H), H_{CH_3} 2.62 (s, 12H), 2.71 (s, 24H) ppm.

[Ru(4-PyT$_3$P)(Py)]$_4$, 3. A spectral grade toluene solution (700 mL) containing [Ru(4-PyT$_3$P)(CO)]$_4$, **2** (32 mg, 1.02×10^{-5} mol), and pyridine (3.5 mL, 4.08×10^{-5} mol) in a Pyrex vessel was photoirradiated using a medium-pressure mercury lamp for 3 h with stirring and vigorous Ar bubbling. The red solution was changed to a brown solution by irradiation. The solution was filtered and evaporated to dryness. The resulting solid was dissolved in a small amount of toluene and separated by an alumina column (activity III) with toluene as an eluent. The first eluted brown band was collected and evaporated to dryness. The resulting deep-purple solid was recystallized from toluene-methanol, and dried at 110 °C in vacuo for 5 h. Yield: 22 mg, 63%. Anal. Calcd for $C_{204}H_{152}N_{24}Ru_4$: C, 73.23; H, 4.64; N, 10.05.

(23) Collman, J. P.; Barnes, C. E.; Brothers, P. J.; Collins, T. J.; Ozawa, T.; Callucci, J. C.; Ibers, J. A. *J. Am. Chem. Soc.* **1984**, *106*, 5151.

Found: C, 73.29; H, 4.69; N, 9.75. ^{1}H NMR ($CDCl_3$, 270 MHz): $H_{2,6-Py}$ 0.93 (d, 5.93 Hz, 4H), 1.91 (d, 7.59 Hz, 4H), $H_{3,5-Py}$ 5.67 (d, 5.93 Hz, 4H), 5.78 (d, 7.59 Hz, 4H), H_β 6.65 (d, 4.62 Hz, 8H), 7.77 (d, 4.62 Hz, 8H), 8.06 (d, 4.62 Hz, 8H), 8.12 (d, 4.62 Hz, 8H), H_o 7.7−7.9 (m, 24H), H_m 7.2−7.4 (m, 24H), H_{CH_3} 2.57 (s, 12H), 2.65 (s, 24H), $H_{\alpha-Py}$ 2.22 (d, 8H), $H_{\beta-Py}$ 4.97 (t, 8H), $H_{\gamma-Py}$ 5.84 (t, 4H) ppm.

Acknowledgment. We acknowledge the funds from a Grant-in-aid for Scientific Research from the Ministry of Education, Science, Sports and Culture, Japan (No. 08454206) and the 1994 Kawasaki Steel 21st Century Foundation.

Supporting Information Available: Figures of H−H COSY of **2** and ^{1}H NMR spectral change of **3** in d_5-pyridine at 90 °C (Figures S1 and S2) (2 pages). Ordering information is given on any current masthead page.

IC970884W